Effect of depolarization on temporal coherence within a focused supercontinuum

Brendan J. Chick, James W. M. Chon, and Min Gu*

Centre for Micro-Photonics, Faculty of Engineering and Industrial Sciences, Swinburne University of Technology, Post Office Box 218, Hawthorn 3122, Victoria, Australia

(Received 10 February 2010; published 20 August 2010)

Under the conditions of vectorial diffraction, an increase in refraction at the extremities of the lens rotates the incident polarization state which transfers energy from the initial state to the orthogonal transverse field and the longitudinal field, which is known as depolarization. Since the field is a vectorial field containing three polarization components, the theory for the degree of coherence is first extended to incorporate cross-correlation effects within these vectorial components which are calculated through a coherency matrix. The use of this matrix provides an insight into interesting correlation effects between copropagating vectorial fields such as the coupled modes (linear polarized modes) of the supercontinuum generated by a photonic crystal fiber. An investigation is presented on the coherence times for the supercontinuum field generated by cross coupling into the photonic crystal fiber. The coherence times under cross-coupling conditions show that the degree of coherence of the two coupled modes from the fiber are different, which is due to the differences in phase. For a supercontinuum with a linear polarization state, the coherence times along the x, y, and z axes are different, with the most significant change occurring along the optical axis (z) where the coherence time changes by an order of magnitude when the numerical aperture is increased from 0.1 to 1.

DOI: 10.1103/PhysRevA.82.023811 PACS number(s): 42.25.Fx, 42.25.Hz, 42.25.Ja, 42.25.Kb

I. INTRODUCTION

The diffraction of a polychromatic wave can be determined by the vectorial diffraction theory using the Debye approximations [1]. The superposition of planes waves originating from the diffraction aperture forms points of singularity where the phase is discontinuous [2,3]. The interaction of the incoming electromagnetic field and these points of singularity redistributes the bandwidth [3], which effects the fields temporal coherence [4]. It has been shown that with an increase in numerical aperture (NA), the singularities no longer exist in particular directions [2]. Coherence, the ability of two fields to maintain a constant phase relation, is important in optics and is the governing principle behind optical interference [5,6], which can be used to quantify changes in the temporal, spectral, and phase relationship of the vectorial field components. When an electromagnetic field is focused by a high-NA lens energy is transferred from the incident polarization state to the transverse orthogonal and the longitudinal field components, which is called depolarization. The transfer of energy due to depolarization is related to a change in coherence, which physically can be quantified through the coherence time of each vectorial component and the coherence time of the cross-correlation between vectorial components. The theoretical treatment of the coherence effects of a vectorial field have been previously investigated by Wolf in 2003 [7] and by Dennis in 2004 [8]. However, these studies only investigated the frequency dependence of an incident polychromatic wave. The extension that is made in this article is to investigate how these correlations influence the temporal aspect of a propagating polychromatic wave such as a supercontinuum (SC) in the focal region of a high-NA lens.

Over the past decade applications which involve diffraction or interference have evolved due to the development of SC [9–12] generation by a microstructured optical fiber [13,14]. An SC is the source of choice for many of these applications because of its broadband characteristics and temporal structure. When an ultrashort pulse is coupled into a photonic crystal fiber (PCF) it is influenced by the balance between the nonlinearity induced by the Kerr effect [15] and the designed dispersion [16] introduced by the photonic crystal structure. Under the condition of the anomalous dispersion [14], the pulse initially compresses and forms a high-order soliton. At a particular point in the evolution the phase shift on the high-order soliton becomes unstable and breaks into many fundamental solitons, known as soliton fission [17,18]. With increasing length, the third order and other higher-order dispersion effects begin to dominate and what forms is a complex temporal and spectral electromagnetic field.

Physically, the spatial and temporal phase coupling which was presented in [4] is not restricted to scalar fields and would manifest as a cross-phase coupling between vectorial field components. Birefringence is an important property of a PCF because it allows the capability of maintaining the polarization state by creating both strong modal guidance and spectrally dependent vectorial field components. The complicated temporal phase associated with the birefringent modes of the SC couples with the spatial phase from the diffraction by the lens [4], which would produce interesting correlations under vectorial diffraction conditions.

The aim of this article is to provide a detailed theoretical description of the temporal coherence of an SC under vectorial diffraction conditions. We present the coherence relationship between the field components produced by depolarization under high-NA diffraction and the relationship between the SC fields produced by highly birefringent PCF when diffracted by a lens of high NA.

*mgu@swin.edu.au

II. THREE-DIMESIONAL VECTORIAL DIFFRACTION MATRIX

For a circular symmetric incident field the diffraction of the field with a horizontal polarization direction can be shown to be given by [1,19]

$$\mathbf{E}^h(v,u,\psi,\omega) = \begin{bmatrix} E_x(v,u,\psi,\omega) \\ E_y(v,u,\psi,\omega) \\ E_z(v,u,\psi,\omega) \end{bmatrix} = \frac{i\omega}{2c}\begin{bmatrix} [I_0 + \cos(2\psi)I_2] \\ \sin(2\psi)I_2 \\ 2i\cos(\psi)I_1 \end{bmatrix}, \quad (1)$$

and for the vertical polarization state is given by

$$\mathbf{E}^v(v,u,\psi,\omega) = \begin{bmatrix} E_x(v,u,\psi,\omega) \\ E_y(v,u,\psi,\omega) \\ E_z(v,u,\psi,\omega) \end{bmatrix} = \frac{i\omega}{2c}\begin{bmatrix} \sin(2\psi)I_2 \\ [I_0 - \cos(2\psi)I_2] \\ 2i\sin(\psi)I_1 \end{bmatrix}, \quad (2)$$

where

$$\begin{bmatrix} I_0 \\ I_1 \\ I_2 \end{bmatrix} = \int_0^\alpha E^i(\omega)\cos^{1/2}\theta\sin\theta \times \begin{bmatrix} (1+\cos\theta)J_0(v\sin\theta/\sin\alpha) \\ (\sin\theta)J_1(v\sin\theta/\sin\alpha) \\ (1-\cos\theta)J_2(v\sin\theta/\sin\alpha) \end{bmatrix} \times e^{iu\cos\theta/\sin^2\alpha}d\theta. \quad (3)$$

Here u and v represent the normalized axial and radial dimensionless parameters of the imaging system given by $u = kz_2\sin^2\alpha$ and $v = kr_2\sin\alpha$. ω is the frequency, c is the speed of light, k is the wave number, ψ is the azimuthal angle, and α is the maximum angle of diffraction. What essentially occurs is the incident polarization rotates slightly to increase the strength of the orthogonal transverse and longitudinal field polarization states. Throughout this article, the results of the analysis of the dimensions of the focal region are presented using the dimensionless coordinates u_0 and v_0. The longitudinal coordinate is given by $u_0 = \frac{2\pi z_2}{\lambda_0}\sin^2\alpha$ and the transverse coordinate is given by $v_0 = \frac{2\pi r_2}{\lambda_0}\sin\alpha$. For an arbitrary polarization angle the diffraction by a lens under conditions of vectorial diffraction is given by

$$\mathbf{E} = a\mathbf{E}^h + b\mathbf{E}^v, \quad (4)$$

where a and b represent the polarization coefficients for the horizontal and vertical polarization states, respectively.

The characterization of the degree of coherence for a vector field $\mathbf{E}(V,t)$ begins with the coherency matrix, which is calculated by

$$g^1_{mn}(V,\tau) = \frac{\langle \mathbf{E}^*_m(V,t)\mathbf{E}_n(V,t+\tau)\rangle}{[\langle|\mathbf{E}_m(V,t)|^2\rangle\langle|\mathbf{E}_n(V,t)|^2\rangle]^{1/2}}, \quad (5)$$

where m and n are the polarization states in the spatial directions x,y, and z, where V represents the collective dimensions of the diffraction volume. For m and $n = x$, g^1 represents the autocorrelation of the electric field component in the x direction. For $m \neq n$, g^1 represents the cross-correlation of the vector components of the field. Physically, this matrix quantifies the transfer of energy between field components and provides the ability to analyze the polarization properties of the degree of coherence for the focal region.

The components of the field for a linear polarization state with an arbitrary polarization angle under vectorial diffraction can be determined by the theoretical formulas by Richards and Wolf in 1959 [19]. When combined these equations form the following set of equations

$$E_x(V,t) = \frac{i\omega}{2c}\{aI_0(V,t) + [a\cos(2\psi) + b\sin(2\psi)]I_2(V,t)\}, \quad (6)$$

$$E_y(V,t) = \frac{i\omega}{2c}\{bI_0(V,t) + [a\sin(2\psi) + b\cos(2\psi)]I_2(V,t)\}, \quad (7)$$

$$E_z(V,t) = \frac{i\omega}{2c}\{2i[a\cos(\psi) + b\sin(2\psi)]I_1(V,t)\}. \quad (8)$$

The vectorial field components, which contribute to the degree of coherence for the x, y, and z axes, are shown in Table I. The degree of coherence for a linear polarization state

TABLE I. Contributions to the field $\mathbf{E}$ for the x, y, and z axes.

axis	ψ	$\mathbf{E}^h$ (units of $i\omega/2c$)	$\mathbf{E}^v$ (units of $i\omega/2c$)	$\mathbf{E}$ (units of $i\omega/2c$)
z	0°	$E^h_x = I_0(z,t) + I_2(z,t)$	$E^v_x = 0$	$E_x = aI_0(z,t) + aI_2(z,t)$
		$E^h_y = 0$	$E^v_y = I_0(z,t) - I_2(z,t)$	$E_y = bI_0(z,t) - bI_2(z,t)$
		$E^h_z = 0$	$E^v_z = 0$	$E_z = 0$
y	90°	$E^h_x = I_0(y,t) - I_2(y,t)$	$E^v_x = 0$	$E_x = aI_0(y,t) - aI_2(y,t)$
	or	$E^h_y = 0$	$E^v_y = I_0(y,t) + I_2(y,t)$	$E_y = bI_0(y,t) + bI_2(y,t)$
	270°	$E^h_z = 0$	$E^v_z = 2iI_1(y,t)$	$E_z = b2iI_1(y,t)$
x	0°	$E^h_x = I_0(x,t) + I_2(x,t)$	$E^v_x = 0$	$E_x = aI_0(x,t) + aI_2(x,t)$
	or	$E^h_y = 0$	$E^v_y = I_0(x,t) - I_2(x,t)$	$E_y = bI_0(x,t) - bI_2(x,t)$
	180°	$E^h_z = 2iI_1(x,t)$	$E^v_z = 0$	$E_z = a2iI_1(x,t)$

with an arbitrary polarization angle in the directions x, y, and z can be determined in terms of the field components I_0, I_1, and I_2.

The set of coherence functions can be used to determine the coherence times of the focus under conditions of vectorial diffraction, which are given by

$$\tau^c_{mn}(V) = \int_{-\infty}^{\infty} \left| g^1_{mn}(V,\tau) \right|^2 d\tau. \tag{9}$$

For a horizontal polarization state ($a = 1$, $b = 0$), the coherence times for the x, y, and z axes are determined by the nonzero components $\tau^c_{xx}(x)$, $\tau^c_{xz}(x)$, $\tau^c_{zx}(x)$, $\tau^c_{zz}(x)$, $\tau^c_{xx}(y)$, and $\tau^c_{xx}(z)$. The rest of the components of the coherence times are equal to zero, which is caused by the polarization coefficient $b = 0$. When the NA is below 0.7 the effects of depolarization can be neglected and the terms I_1 and $I_2 = 0$. Under these conditions the field E reduces to a scalar field determined by I_0, where the degree of coherence and the coherence time are given by

$$g^1_{mn}(V,\tau) = g^1_{xx}(V,\tau) = \frac{\langle I_0(V,t) I_0(V,t+\tau)\rangle}{[\langle |I_0(V,t)|^2\rangle \langle |I_0(V,t)|^2\rangle]^{1/2}}, \tag{10}$$

$$\tau^c_{xx}(V) = \int_{-\infty}^{\infty} \left| g^1_{xx}(V,\tau) \right|^2 d\tau, \tag{11}$$

respectively.

Consider the general case of a hyperbolic secant with a pulse duration of 0.1 ps. The coherence time for an NA = 0.1 under the vectorial diffraction conditions is shown in Fig. 1, which gives an identical result to the coherence time produced by the Fresnel diffraction [4]. Under high-NA vectorial diffraction conditions the coherence of the field is no longer effected by the point of destructive interference, which is due to depolarization.

The final mathematical analysis involves an incident field with a polarization orientation at 45°. The diffraction by the lens under vectorial diffraction conditions is given by

$$\mathbf{E}_{45} = \mathbf{E}^h + \mathbf{E}^v = \frac{1}{\sqrt{2}} \begin{bmatrix} E^h_x \\ E^h_y \\ E^h_z \end{bmatrix} + \frac{1}{\sqrt{2}} \begin{bmatrix} E^v_x \\ E^v_y \\ E^v_z \end{bmatrix}. \tag{12}$$

When diffracted by a high NA the degree of coherence for the field $\mathbf{E}_{45}$ becomes complicated. For this investigation the degree of coherence is calculated for only the optical axis where the coherence matrix is given by

$$g^1(z,\tau) = \begin{bmatrix} g^1_{xx}(z,\tau)\ g^1_{xy}(z,\tau) \\ g^1_{yx}(z,\tau)\ g^1_{yy}(z,\tau) \end{bmatrix}. \tag{13}$$

The coherence times generated by the degree of coherence for $\mathbf{E}_{45}$ is given by

$$\tau^c_{mn}(z) = \begin{bmatrix} \tau^c_{xx}(z)\ \tau^c_{xy}(z) \\ \tau^c_{yx}(z)\ \tau^c_{yy}(z) \end{bmatrix}. \tag{14}$$

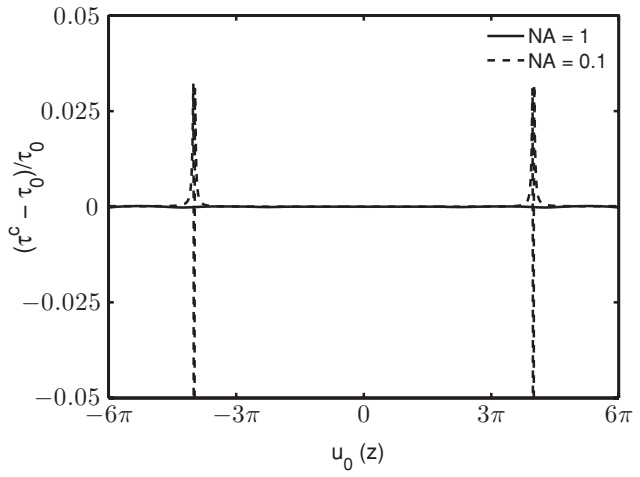

FIG. 1. A comparison between the coherence times for a lens of NA = 1 and 0.1 with hyperbolic secant ultrashort pulse with a width of 0.1 ps.

III. VECTORIAL DIFFRACTION OF A SUPERCONTINUUM

A. Supercontinuum generation

The mathematical method used to simulate the SC field [20] uses the coupled-mode nonlinear Schrödinger equation. The dipsersion and the nonlinear properties of the nonlinear PCF have been modeled previously and can be obtained from Chick *et al.* [20]. The numerical procedure of calculating the SC field is the split-step Fourier method [21] using an adaptive propagation step size implemented through a local error method. The typical temporal window used to contain the SC wave was 6 picoseconds with a resolution of 2^{13}. The input power and pulse width of the incident pulse were 3000 W and 0.1 ps, respectively. The numerical approach is consistent with well-known articles on SC generation [17,21] and has been presented in a previous article by Chick *et al.* [20]

B. Linear polarization

For a linear polarization state the degree of coherence and the coherence time are determined by the previous theoretical derivations. It is expected that the coherence times for the autocorrelation of the electric field in the direction of the incident polarization state E_x would be influenced by the points of destructive interference. The coherence time for the SC diffraction by a lens is shown in Fig. 2 for the x, y, and z axes. The input polarization state to the PCF is in the x direction and the analysis is for the autocorrelation of the field component E_x determined by Eq. (9). Figure 2 shows three key effects: the influence of the spatial phase through the points of destructive interference on the field; the reduction of the coherence time with increased NA; and a lateral (x and y axes) and a longitudinal (z axis) shift in the coherence time. The gradual shift inward (y) and outward (x) is due to the change in superposition of the wave as it passes through the lens. The modification of the field by the spatial phase associated with the lens changes the field E_x to become slightly asymmetric, which is only seen under higher-NA conditions. Along the optical axis a more significant change occurs and is due to the superposition condition no longer forming points

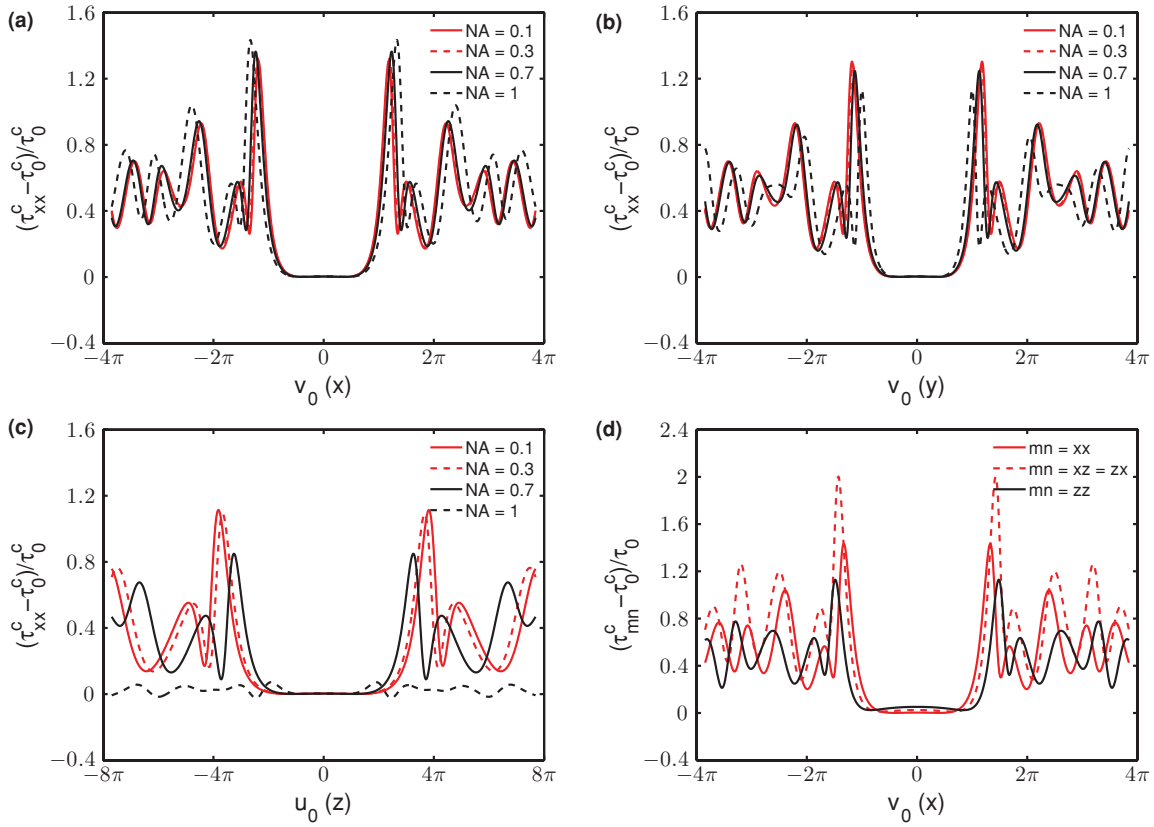

FIG. 2. (Color online) The coherence time for the diffraction by a lens of varying NA along the (a) x, (b) y, and (c) z axes. These coherence times are calculated for the autocorrelation of the electric field in the direction of the $\mathbf{E}^i$ (E_x). (d) The coherence times for the diffraction by a lens of NA $= 1$ along the x axis, which contains the autocorrelation and cross-correlation coherence times with respect to the E_x and E_z fields.

of destructive interference under higher-NA conditions. The coherence time for a NA $= 0.1$ is identical to the coherence time obtained for the stationary observation frame shown by Chick *et al.* [4].

For the transverse axis x, the field component $E_z \neq 0$ leading to a coherency matrix containing cross-coupling correlation terms between E_x and E_z. Figure 2(d) shows the coherence times simulated using Eq. (9). The interesting observation is that the coherence time generated by the cross coupling of the field components ($mn = xz$) is not a simple superposition of the coherence times generated by the autocorrelations ($mn = xx$ and $mn = zz$). This effect is understandable because the correlation is dependent on the phase structure of each component of the incident field and the transfer energy due to depolarization. Effectively, the

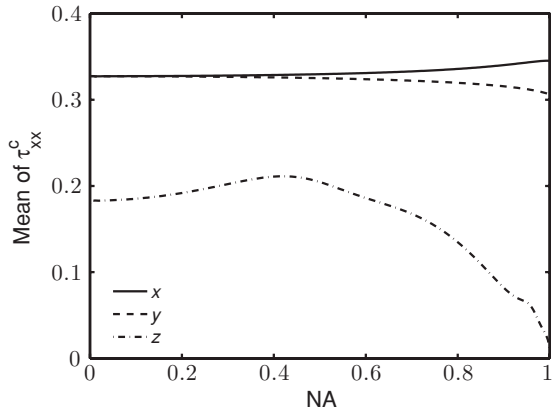

FIG. 3. The mean coherence time of an SC as a function of NA for the x, y, and z axes.

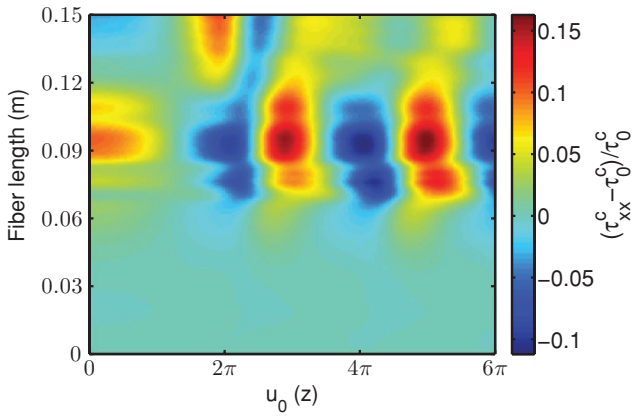

FIG. 4. (Color online) The coherence time of the autocorrelation of the diffraction by a lens of NA $= 1$ the electric field E_x with variation in the fiber length.

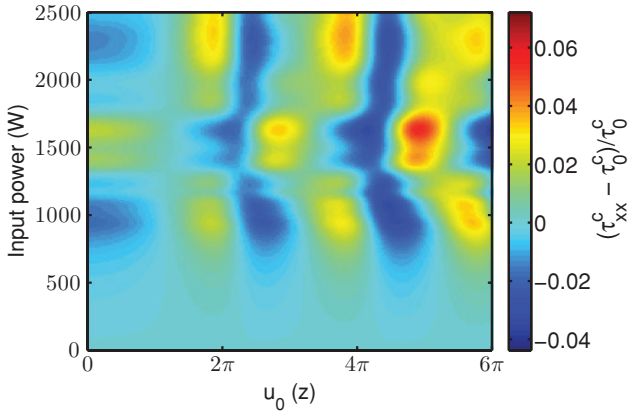

FIG. 5. (Color online) The power dependence of coherence time in the focus of a NA = 1 lens for input fields generated by the nonlinear PCF of varying input power. The coherence time is for a linear polarized field orientated along the x direction.

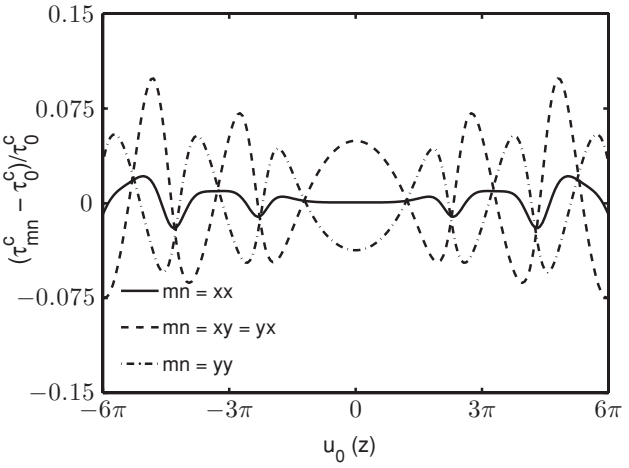

FIG. 7. The coherence time for the autocorrelations and cross-correlations calculated for the diffraction by a lens of NA = 1 along the optical axis.

coherence time formed by the cross coupling between the polarization states is a measure of the longevity of the elliptical polarization produced by depolarization.

The influence of the NA can be quantified by calculating the mean of the coherence time as a function of NA and is shown in Fig. 3. By increasing the NA, there exists a redistribution of energy within the E_x component from the y axis to the x axis, which alters the degree of coherence of the field. Along the optical axis the change in the degree of coherence is different as there no longer exists points of destructive interference, leading to a change in the mean coherence time by an order of magnitude from low NA (0–0.4) to the high NA (1).

Since the SC field is generated by an accumulation of phase associated with nonlinearity and dispersion, it becomes important to assess how the degree of coherence changes with phase under vectorial diffraction conditions. A method for analyzing this change is by calculating the diffraction of the

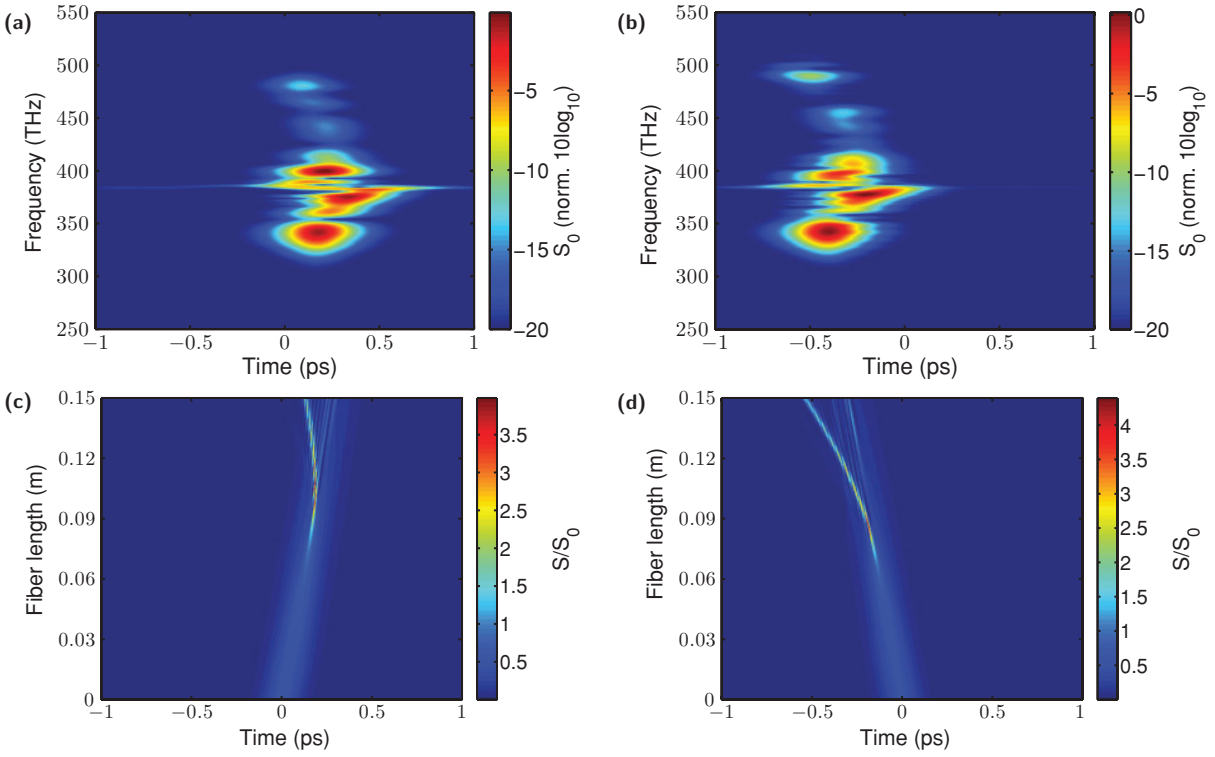

FIG. 6. (Color online) The PCF output field for an incident polarization state at 45°. Figure (a) the horizontal (x) polarization state, (b) the vertical (y) polarization state, (c) the horizontal (x) polarization state as a function of fiber length, and (d) the vertical (y) polarization state as a function 2 of fiber length.

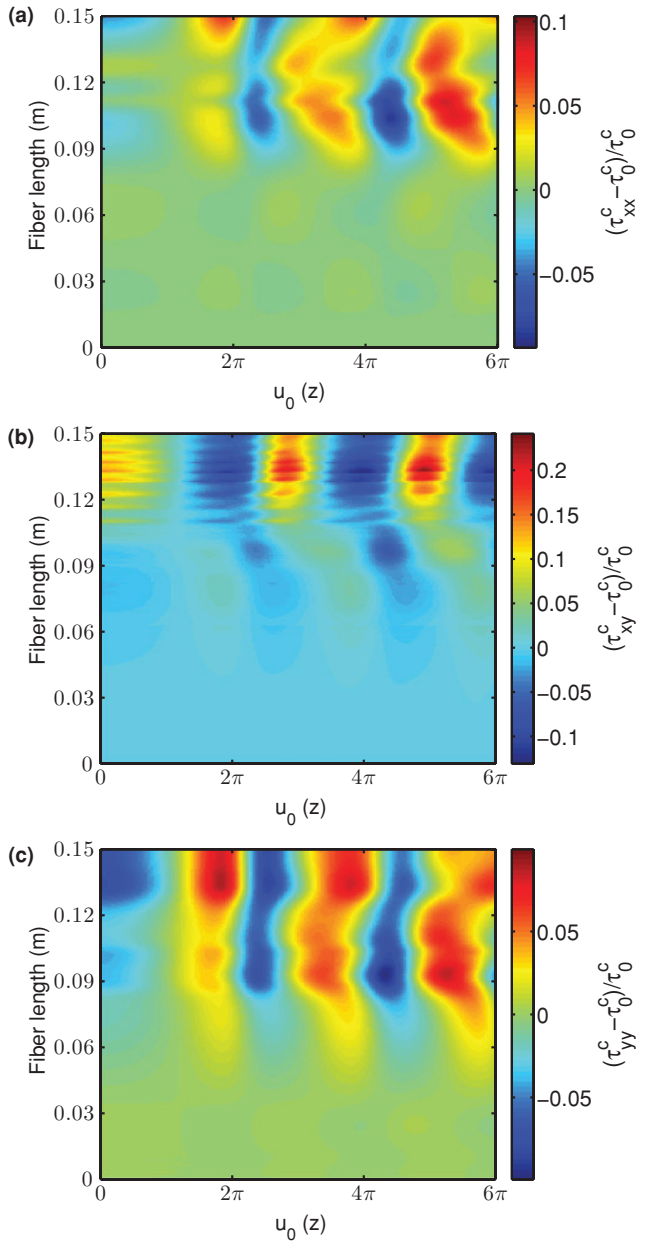

FIG. 8. (Color online) The coherence time for the autocorrelations and cross-correlations calculated for the diffraction by a lens of NA = 1 as a function of fiber length along the optical axis. (a) Coherence time produced by the autocorrelation of E_x; (b) coherence time produced by the cross-correlation E_x and E_y; and (c) coherence time produced by the autocorrelation of E_y.

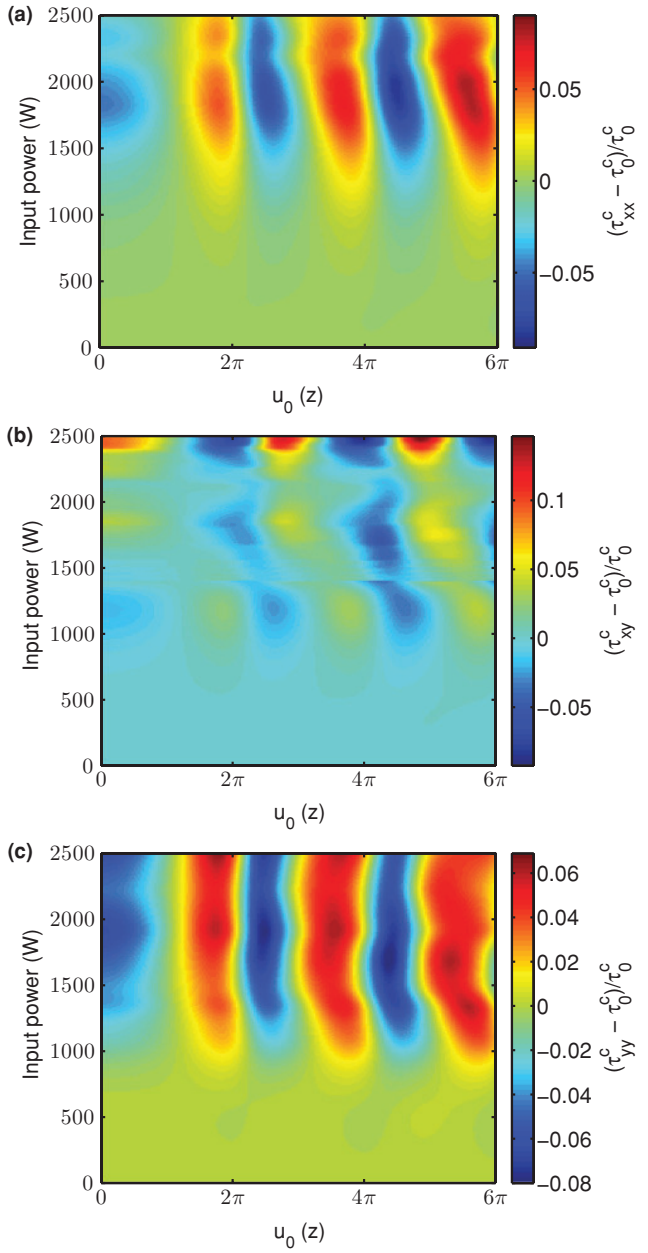

FIG. 9. (Color online) The coherence time for the autocorrelations and cross-correlations calculated for the diffraction by a lens of NA = 1 as a function of the input power along the optical axis. (a) Coherence time produced by the autocorrelation of E_x; (b) coherence time produced by the cross-correlation E_x and E_y; and (c) coherence time produced by the autocorrelation of E_y.

SC produced by a variation in fiber length (Fig. 4) along the optical axis of the focal region of a lens of NA = 1 and is shown in Fig. 4. As the initial ultrashort pulse travels through the optical fiber it accumulates phase which changes the spectral and temporal components. There exists a point in the evolution where the temporal coherence dramatically changes which is due to the formation and annihilation of a high-order soliton.

The degree of coherence is dependent on the input power to the PCF and is shown in Fig. 5. For low input powers the variation in coherence time is low, which occurs because the phase on the pulse is dominated by dispersion effects. With increased power, the coherence time is expected to change since with the increased dominance of nonlinearity. The higher input power increases the initial order of the soliton which then after fission changes the degree of coherence, which enhances the coherence time.

The results contained in this article, thus far, have been in accordance with previous literature and are consistent with a previously published article by Chick *et al.* in 2009 [4].

For example, the coherence times shown in Figs. 1 and 3 are consistent with the coherence times of the stationary reference frame presented in Ref. [4]. The numerical procedure for the SC is in agreement with scientifically accepted literature [17] and is consistent with a previous article by Chick *et al.* in 2008 [20]. The methodology is now used to understand the interaction between coupled modes in SC generation under conditions of vectorial diffraction.

C. Coupled-mode propagation

So far the analysis has been restricted to a linear incident polarization state, which emphasises the depolarization inherent from a high-NA lens. The coupled-mode nonlinear Schrödinger equation allows the ability to simulate an SC field with a polarization orientation at 45° which can occur in highly birefringent PCF. The output spectrograms of the SC field emerging from a highly birefringent PCF is shown in Fig. 6. The field was generated using the dispersion and nonlinear parameters discussed by Chick *et al.* [20] with a pulse duration of 100 fs and a peak power of 2500 W. Also shown is the propagation of the ultrashort pulse along the fiber with a length of 0.15 m.

In the focal plane of the lens, these coupled modes should affect the coherence matrix and the coherence times. Figure 7 shows the coherence times produced from Eq. (14). It is evident that the coherence time for the cross-correlation between the modes is no longer the superposition between the autocorrelated fields and occurs because of their nonconstant relative phase.

The phase due to nonlinearity and dispersion can be isolated along the fiber length to understand the influence of polarization on the degree of coherence. Figure 8 shows the polarization coherence times occurring due to the coupled modes of the PCF along the optical axis as a function of the fiber length. The autocorrelations behave in the same manner as depicted in Figs. 4 and 5, the degree of coherence changes with input phase. The cross-correlated degree of coherence in Fig. 8(b) shows modulations which occur due to the differences in phase between the fibers modes. The soliton fisson dynamics in SC generation contains spectral expansion and contractions processes. The differences between the soliton fluctuations of the fiber modes could be attributed to the modulations shown in the cross-correlated degree of coherence and the coherence time in Fig. 8(b). In both cases of a linear polarized SC field and a 45° polarized SC field, the coherence time has a greater variance after the formation of the soliton and the rapid spectral expansion of the SC field. After this point, the coherence within the focal region becomes dominated by interference between dispersive waves and the fundamental solitons.

The expansive spectral features of an SC can only be obtained by coupling an ultrashort pulse of sufficient power to instigate the formation of solitary waves. The effects of temporal phase on the focal region can also be analyzed by observing the change in coherence time as a function of input power to the PCF (Fig. 9). At low input powers, the output spectra of the PCF is dominated by the dispersion of the fundamental solitons and under these conditions the phase accumulated through propagation is relatively simple. The cross coupling between the focused coupled modes in this case is shown as a small change in coherence time. With the increase in input power the SC is formed by the amalgamation of nonlinear and dispersive processes, and as expected rapidly expands the bandwidth. The cross coupling between the focused coupled modes becomes complicated because of the superposition of their differing phase, which results in subtle changes in the coherence time [Fig. 9(b)].

IV. CONCLUSION

In summary, the optical field components occurring because of depolarization by the diffraction of a high-NA lens reduce the coherence time along the optical axis which is attributed to the superposition of the wave front no longer forming points of destructive interference. Under conditions of vectorial diffraction, the mean coherence time will change by an order of magnitude when the NA changes from a low NA (0–0.4) to a high NA of 1. For the transverse axes the mean coherence time increases and decreases in the x direction and y directions, respectively, which is also due to depolarization.

When considering the case of a vectorial field, the components of the field create interesting cross-coupling characteristics, which are determined by a coherency matrix. When the SC modes of a highly birefringent PCF are focused by a high-NA objective, the coherence times produced by their autocorrelations are different due to the phase differences between the modes. In addition, the coherence time for the degree of coherence between these two modes (cross-coupled coherence time) is significantly different. In these cases of autocorrelation and cross-correlation the temporal phase is significantly contributing to the degree of coherence in the focal region, to such an extent that the phase difference between the two modes creates strong changes in the coherence times.

ACKNOWLEDGMENTS

The authurs thank the Australian Research Council for its financial support. Brendan Chick thanks the Australian Cooperative Research Centre for polymers and for their scholarship support.

[1] M. Gu, *Advanced Optical Imaging Theory* (Springer Velag, Heidelberg, Germany, 2000).

[2] G. Gbur, T. D. Visser, and E. Wolf, Phys. Rev. Lett. **88**, 013901 (2001).

[3] D. Ganic, J. W. M. Chon, and M. Gu, Appl. Phys. Lett. **82**, 1527 (2003).

[4] B. J. Chick, J. W. M. Chon, and M. Gu, Opt. Express **17**, 20140 (2009).

[5] L. Mandreal and E. Wolf, *Optical Coherence and Quantum Optics* (Cambridge University Press, Cambridge, England, 1995).
[6] R. Loudon, *The Quantum Theory of Light*, 3rd ed. (Oxford University Press, Oxford, England, 2000).
[7] E. Wolf, Phys. Lett. A **312**, 263 (2003).
[8] M. R. Dennis, J. Opt. A **6**, S26 (2004).
[9] I. Hartl, X. D. Li, C. Chudoba, R. K. Ghanta, T. H. Ko, J. G. Fujimoto, J. K. Ranka, and R. S. Windeler, Opt. Lett. **26**, 608 (2001).
[10] H. N. Paulsen, K. M. Hilligsøe, J. Thøgersen, S. R. Keiding, and J. J. Larsen, Opt. Lett. **28**, 1123 (2003).
[11] T. Udem, R. Holzwarth, and T. W. Hänsch, Nature (London) **416**, 233 (2002).
[12] J. E. Morris, A. E. Carruthers, M. Mazilu, P. J. Reece, T. Cizmar, P. Fischer, and K. Dholakia, Opt. Express **16**, 10117 (2008).
[13] J. C. Knight, J. Broeng, T. A. Birks, and P. S. J. Russell, Science **282**, 1476 (1998).
[14] J. K. Ranka, R. S. Windeler, and A. J. Stentz, Opt. Lett. **25**, 25 (2000).
[15] R. H. Stolen and C. Lin, Phys. Rev. A **17**, 1448 (1978).
[16] W. H. Reeves, D. V. Skryabin, F. Biancalana, J. C. Knight, P. S. J. Russell, F. G. Omenetto, A. Efimov, and A. J. Taylor, Nature (London) **424**, 511 (2003).
[17] J. M. Dudley, G. Genty, and S. Coen, Rev. Mod. Phys. **78**, 1135 (2006).
[18] A. V. Husakou and J. Herrmann, Phys. Rev. Lett. **87**, 203901 (2001).
[19] B. Richards and E. Wolf, Proc. R. Soc. A **253**, 358 (1959).
[20] B. J. Chick, J. W. M. Chon, and M. Gu, Opt. Express **16**, 20099 (2008).
[21] G. P. Agrawal, *Nonlinear Fiber Optics*, 3rd ed. (Academic, San Diego, CA, 2002).